ORIGINAL PAPER

Rock Cracking Indices for Improved Tunnel Support Design: A Case Study for Columnar Jointed Rock Masses

Xia-Ting Feng[1] · Xian-Jie Hao[1] · Quan Jiang[1] · Shao-jun Li[1] · John A. Hudson[2]

Abstract Measurements indicate that the development of cracking is a key feature relating to the strength and collapse of a columnar jointed rock mass. In this context, a new support design method utilising rock cracking indices for columnar jointed rock mass under high stress is proposed to restrain the development of cracking in the surrounding rock mass. The method involves limiting the cracking evolution of the surrounding rock mass by designing the appropriate parameters and time of installation of the support system. Two indices are suggested: the allowable depth of the excavation damaged zone (EDZ); and the allowable damage extent of the rock mass in the EDZ. The method involves limiting the evolution of cracking in the surrounding rock mass by designing the parameters and time of installation of the support system. The support system should have a suitable stiffness and installation time so as to restrain the evolution of the depth and damage extent of the EDZ within the surrounding rock. Therefore, the depth and damage extent of the EDZ, as well as the axial stress in the anchor bolts, are calculated at different distances between the support location and the tunnel working face to find the appropriate stiffness and installation time of the support system. The method has been successfully adopted to determine the thickness of shotcrete, the arrangement and installation time of rockbolts, and other parameters, for five large diversion tunnels at the Baihetan hydropower station, China, which were excavated in columnar jointed rock masses.

Keywords Support design method · Rock cracking indices method · Hard rock · Tunnel · Support parameters · Support installation time

1 Introduction

There have been extensive efforts in developing methods for the design of support systems in rock masses consisting of rockbolts/anchors, shotcrete for tunnels and caverns, such as the semi-empirical method (Bhawani et al. 1995), quality control method (Claudio and Gunnar 2004), Q system (Barton et al. 1981), RMR system (Jalalifar et al. 2014), etc. Also, the convergence–confinement method has proved instructional in the context of determination of the support time for an underground tunnel (Pacher 1964; Feder and Arwanitakis 1976; Carranza-Torres and Fairhurst 2000). These efforts have been made to achieve satisfactory support for soft and hard rock tunnels. For nearly half a century of engineering application such methods have been widely used in many slopes, tunnels, and in mining engineering with favourable outcomes (Kalman 2003a, b; Alejano et al. 2010).

In recent years, studies of some deeply buried tunnels have indicated that the failure modes of hard rock masses under high in situ stress are generally as follows: spalling, rock-bursting, stress and stress-structure-induced collapses, which are caused by progressive cracking (Martin et al. 1997; Martino and Chandler 2004; Kulatilake et al. 2004; Chen et al. 2011; Jiang et al. 2013). In addition, according to results from the long-term monitoring of deep tunnels, although cracking within the EDZ in a hard rock mass increases continuously before its entire failure, the displacements are small, and even

✉ Xia-Ting Feng
  xtfeng@whrsm.ac.cn; xia.ting.feng@gmail.com

[1] State Key Laboratory of Geomechanics and Geotechnical Engineering, Institute of Rock and Soil Mechanics, Chinese Academy of Sciences, Wuhan 430071, China

[2] Department of Earth Science and Engineering, Imperial College, London, UK

negligible for engineering purposes. However, the cracking within a hard rock mass (*i.e.*, the development of the EDZ) is the cause of the macroscopic displacement, which result in overall failure (Horii and Nemat-Nasser 1986; Hajiabdolmajid et al. 2002; Golshani et al. 2006). Therefore, the control of the cracking becomes more important in deeply buried, hard rock tunnels. If the cracking of a rock mass is not effectively controlled, stress-induced failure is likely to occur. (Hahn and Holmgren 1979; Gong et al. 2007). For example, the diversion tunnels excavated in a columnar jointed rock mass in the Baihetan Hydropower Station, China, were supported by rockbolts of 6 m in length. However, the depth of excavation damaged zone (EDZ) in the surrounding rock actually extended to 7–9 m, and even to 10 m in some zones and collapse occurred (Wu et al. 2010; Hao et al. 2015).

The key point is that strong rock can have specific unloading mechanical properties which lead to progressive brittle failure (Martin et al. 1997; Cai and Kaiser 2005; Hoek and Martin 2014). Thus, the formation of the EDZ and the evolution of cracking are important concerns for the safety of hard rock tunnels (Hajiabdolmajid et al. 2002; Cai et al. 2004; Pan et al. 2012; Li et al. 2012a, b). It follows, therefore, that a reasonable support design for such strong rock masses, such as columnar jointed rock masses, should be based on their cracking characteristics.

Therefore, the support of a columnar jointed rock mass is studied here with a view to studying the prevention of failure by spalling, or collapse induced by stress and the work reported here proposes a new support design method to restrict the development of cracking and the damage extent of the columnar jointed rock mass in the Baihetan hydraulic project, China. First, the geological conditions and stability problems in a columnar jointed rock mass at the Baihetan Hydropower Station, China are introduced. Second, the principle of the support design based on restraining the cracking and damage process is explained and an index to evaluate cracking and the damage extent of a columnar jointed rock mass is investigated. On this basis, the diversion tunnels excavated in the columnar jointed rock mass are designed for the support parameters and installation time with a shotcrete layer and rockbolts using the proposed approach. The support effect is shown to be verified by acoustic wave testing results. Finally, the convergence-confinement method is compared with the cracking-restraint method.

2 Engineering Background

2.1 Diversion Tunnels in Columnar Jointed Rock Mass

There are five diversion tunnels at the Baihetan Hydropower Station, China, located on the right and left banks of the Jinsha river, indicated by nos. 1–5 (see Fig. 1). Each diversion tunnel has a cross-sectional size of 19 m × 24 m (width × height) and is excavated in columnar jointed basalt having three layers with heights 9.2, 10 and 5 m. There are three types of joints in the columnar rock mass: joints between columns; sub-vertical joints inside a column; and sub-horizontal joints inside a column—as shown in Fig. 2 and termed types I, II and III, respectively (Jiang et al. 2014).

2.2 Stability Problems

After excavation of the first layer, a considerable amount of collapse occurred. Also, the in situ measured results indicated that there was strong time-dependent, cracking behaviour and three stages of EDZ depth evolution were experienced: deceleration, stabilization and acceleration (Hao et al. 2015), see Fig. 3. Thereafter, the cracking-restraint method was used for the support design of the diversion tunnels.

To investigate the deformation, cracking, and damage characteristics of the columnar jointed rock mass surrounding the diversion tunnels subject to high in situ stress, several monitoring methods (such as the multipoint displacement meter, digital borehole camera, and acoustic velocity testing) were used. The results have indicated the following processes. On unloading the high stress after tunnel excavation, the columnar jointed rock mass generates new cracks. For example, a series of annular cracks were generated which were parallel to the sidewall of the diversion tunnel, as shown in Fig. 4a. The testing results from the digital borehole televiewer indicated that the existing cracks in the surrounding hard rock could be opened, closed, or could expand with time—as could newly developed cracks also—revealing different deformation characteristics of the columnar jointed rock mass, such as large or small deformations, stable deformations or an increase of deformation, etc. The data illustrated in Fig. 4a, b, show measurements made at different dates
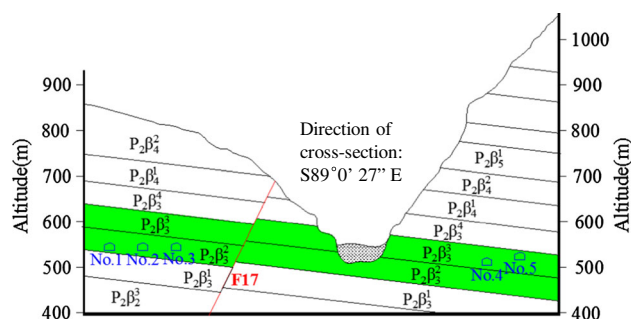

Fig. 1 Stratigraphic distribution of a columnar jointed rock masses and the positions and layout of diversion tunnel nos. 1, 2, 3, 4, and 5. $P_2\beta_3^3$ is the columnar jointed rockmass

Fig. 2 Characteristic of the columnar jointed rock mass **a** joint type and **b** joint network
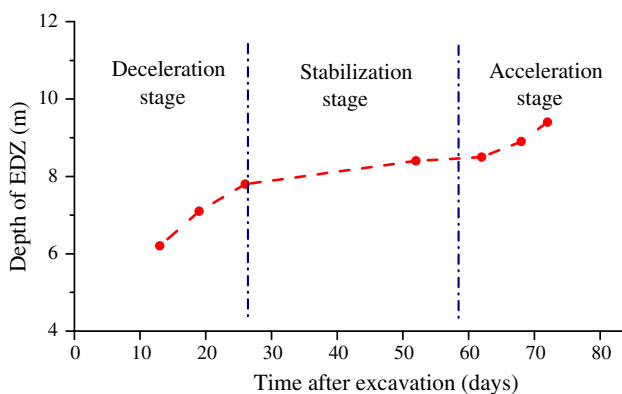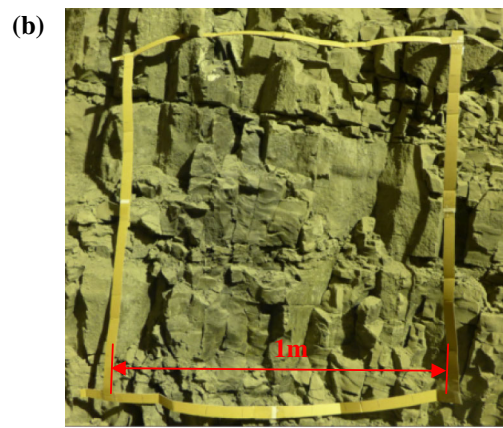

(a)

Type I joints: joints between columns
Strength criterion: Barton-Bandis

Type II joints: approximately vertical joints inside column
Strength criterion: Barton-Bandis

Type III joints: approximately horizontal joints inside column
Strength criterion: Mohr-Coulomb
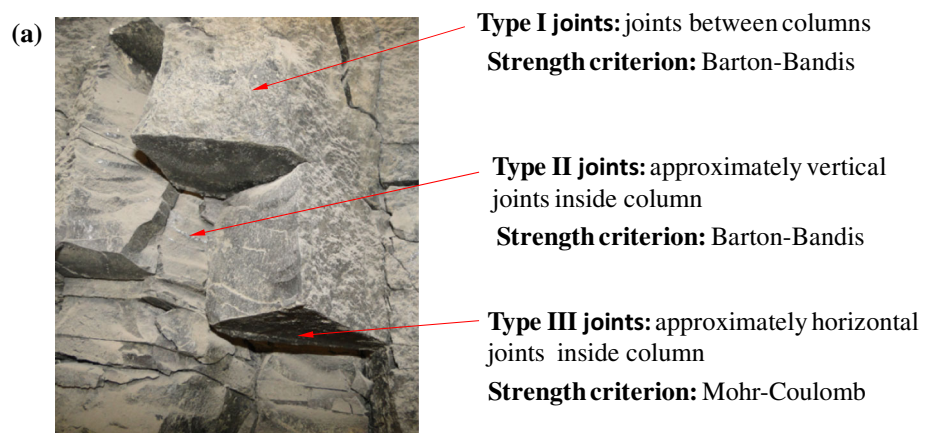

(b)

1m

Fig. 3 Time dependent EDZ evolution at the cross section a chainage K1 + 050 of No. 5 diversion tunnel in the right bank of Jinsha River. It indicated all three stages of EDZ development: deceleration, stabilization and acceleration

using a digital borehole televiewer. Figure 4c indicates that deformation evolved with the excavation progress and time, and then stabilised, with the deformation at the cross-section at chainage K1 + 065 being smaller than at that at chainage K1 + 080. This was due to the fact that there were more cracks at chainage K1 + 080. Sometimes, there

existed no co-ordination between the evolution of the deformation and the evolution of the depth of the EDZ for this columnar jointed rock mass: the depth of the EDZ was not changed significantly, but the deformation of the surrounding rock still increased with time; or the deformation of the surrounding rock was stable but the depth of the EDZ still increased, see Fig. 5 as an example. The testing results described above indicated that there needs to be development of a reasonable design method for determining the support system by considering the characteristics of deformation and cracking of the rock mass under a condition of high initial geostress.

3 Cracking-Restraint Method for Support Design and Its Application to Columnar Joints

3.1 Principle of the Cracking-Restraint Method

The key factor in the cracking-restraint method for support design is use of the support system, including rockbolts, shotcrete, mesh and others, to restrain cracking of the surrounding rocks to avoid collapse. Two indices are used
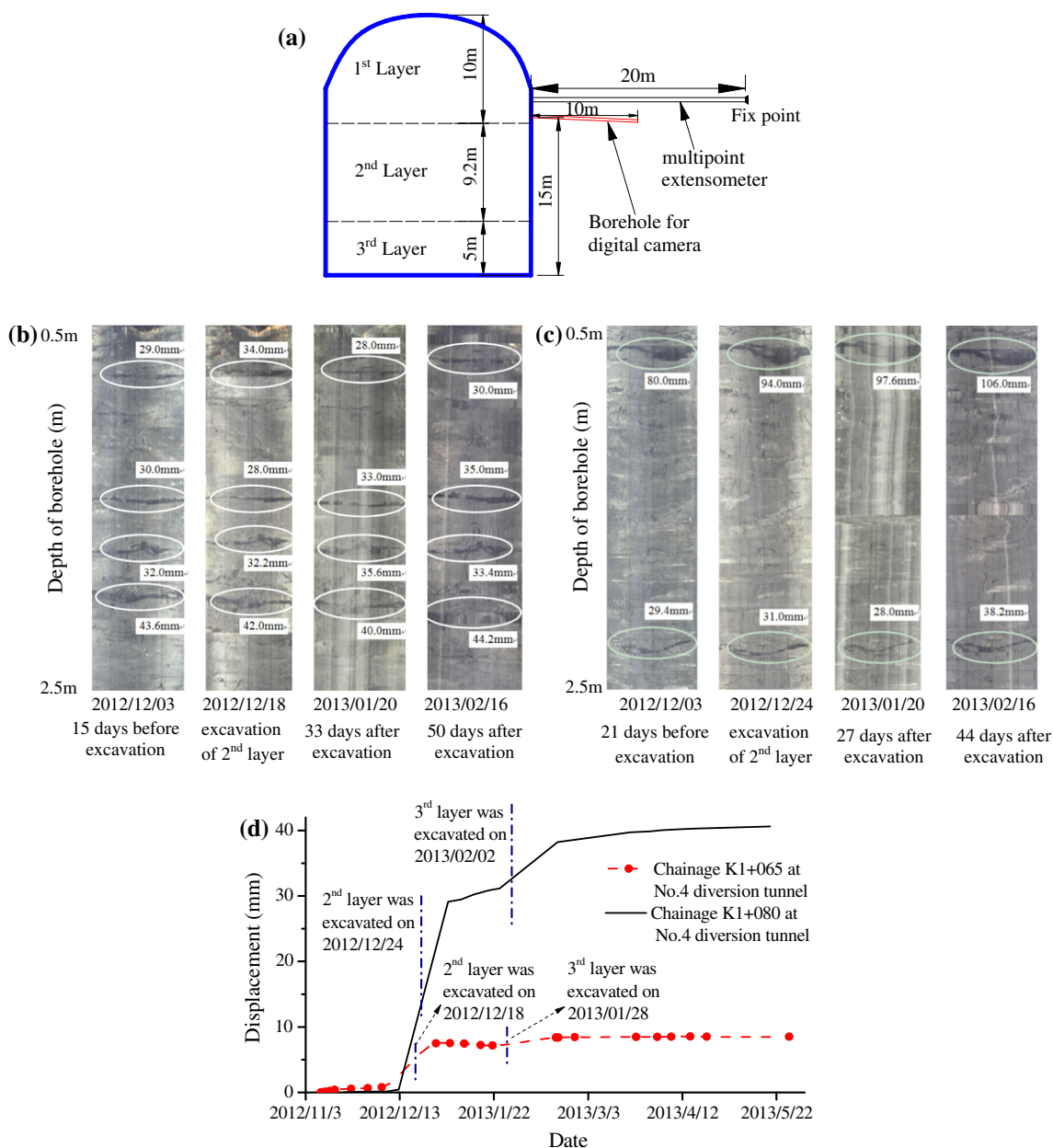
Fig. 4 **a** Layout of drilled boreholes for digital borehole camera and multipoint extensometer for Chainage K1 + 065 and K1 + 080 at No. 4 diversion tunnel, Baihetan Hydropower Station. The monitored evolution of cracking of surrounding rock at **b** chainage K1 + 065 and **c** chainage K1 + 080 in the No. 4 diversion tunnel, Baihetan Hydropower Station. The data at (**b**, **c**) are maximum width of cracks at different time. **d** The monitored deformation evolution of surrounding rock at chainage K1 + 065 and chainage K1 + 080 in the No. 4 diversion tunnel, Baihetan Hydropower Station

for indicating allowable cracking evolution of the surrounding rocks:

- One is the allowable depth of the excavation damage zone, EDZ; and
- The other is the allowable damage extent of the EDZ in the surrounding rock.

The EDZ can be defined as the zone where the rock mass properties change upon excavation. In this research,

acoustic velocity testing was used to delineate the EDZ. The zone where the P-wave velocity decreased was used to delineate the EDZ by comparing images measured before, and after, excavation. The depth of the EDZ can be defined as the distance from the turning point of P-wave velocity curve to the tunnel wall. The extent of the damage within the EDZ can be defined as the decrease amount in P-wave velocity relative to that in the undisturbed rock mass. Using these concepts, the design method controls the depth and
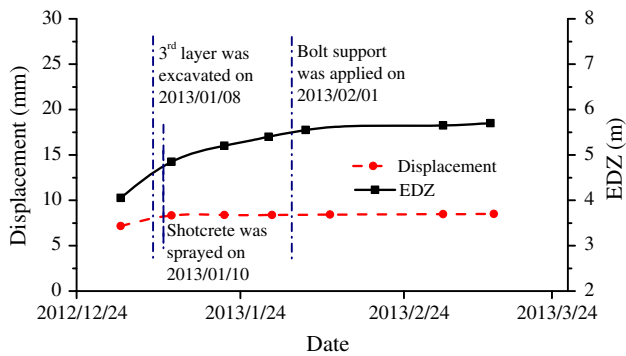
Fig. 5 Significant time-dependent increase in EDZ and insignificant time-dependent increase in displacement at chainage K1 + 065, the No. 4 diversion tunnel, Baihetan Hydropower Station, China

damage extent of the EDZ in the surrounding rocks to an allowable range by installing a support system with a given stiffness at a reasonable distance from the tunnel working face and at a given time after excavation of the tunnel. Figure 6 shows the principle of the support design method. The case where the support system, with lack of stiffness and later installation, is indicated by a in Fig. 6. In this case, neither the evolution of the EDZ depth nor the increase of the damage extent in the surrounding rocks is restrained, see A in Fig. 6. Here, rockbolts have a lower load and do not function sufficiently to restrain cracking in the surrounding rocks. In the case where there is a support system with higher stiffness and earlier installation, indicated by c in Fig. 6, this also does not restrain evolution of the EDZ depth, nor increase in the damage extent of EDZ
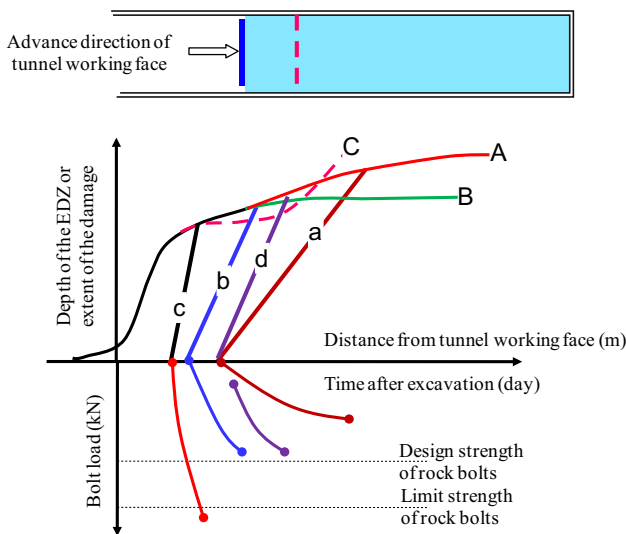
in the surrounding rocks, see C in Fig. 6. This would result in failure of the support system through overloading. Only the support systems indicated by b and d, which have reasonable stiffness and installation time, can restrain evolution of the depth and damage extent in the EDZ in the surrounding rocks, see B in Fig. 6.

3.2 An Index for Evaluating the Damage Extent of the EDZ in the Surrounding Rock Mass

An index for approaching failure, termed the FAI, has been developed to evaluate the extent of yielding or damage of surrounding rocks (Feng et al. 2013). FAI is developed to estimate the cracking extent in a hard rock mass which can be at different stress–strain stages, as shown in Fig. 7. Before yielding, the ratio of the distance from the current stress state to the yield surface and that of hydrostatic pressure can be used to characterize the FAI. After yield, the equivalent plastic strain is usually used to characterize it. FAI corresponds to points along the stress–strain curves for the rock: i.e., the FAI values of 0, 1, 2, represent respectively the initial point, peak strength point and residual strength point on the stress–strain curve of the rock mass. For hard rock, under high stress, the initiation and propagation of stress-induced crack damage is a precursor in all brittle failure of rocks (Martin 1993). According to indirect monitoring methods, such as acoustic emission
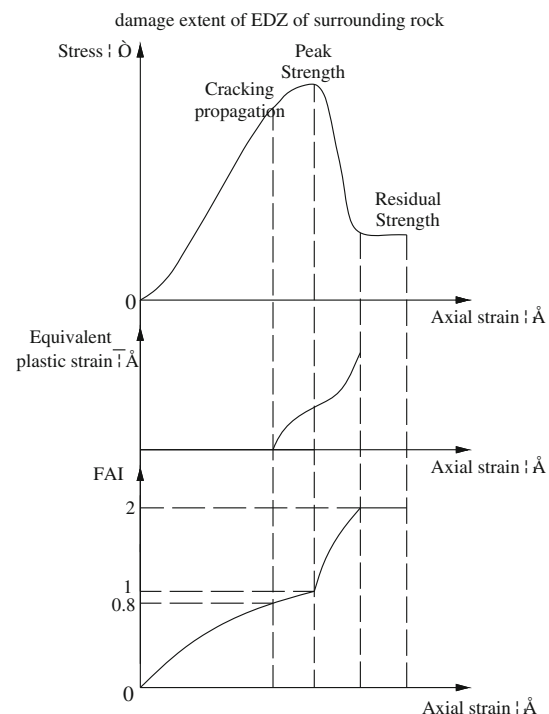

Fig. 6 Determination of appropriate support time and parameters using the method to restrain cracking/EDZ of the surrounding rocks. The *lines a–d* indicate support characteristic curves. The *lines A–C* indicate characteristic curves of depth and damage extent of EDZ of surrounding rock

Fig. 7 Stress–strain curve of hard rock and its corresponding equivalent plastic strain and FAI value

(AE), and micro-seismic (MS) monitoring, the crack coalescence shown in Fig. 7 usually starts at stress levels approximately 0.7–0.8 times the peak strength (Martin et al. 2001; Cai et al. 2004). For columnar jointed rock masses, which suffer significant time-dependent cracking, the boundary of the EDZ is such that $0.8 < \text{FAI} < 1$, which corresponds to points of crack propagation along the stress–strain curves shown in Fig. 7.

3.3 Development of the FAI for the Columnar Jointed Rock Mass

The elastic-brittle-plastic constitutive model is used to describe the characteristics of basalt rock. It incorporates deformation, behaviour, and strength criteria. Three sets of columnar joints, with different dips and dip directions, can form different cross-sections, including triangular, quadrangular, pentagonal, hexagonal, etc. The elastic behaviour of a rock mass containing multiple joints includes the elastic deformation of both intact rock and joints. Considering the highly transverse characteristics of columnar jointed rock mass, the transverse stiffness matrix is selected to represent this anisotropy. Because Type I and II joints have rough joint surfaces, as shown in Fig. 2, the Barton–Bandis shear strength is used to describe their non-linear mechanical behaviour; however, Type III joints have smooth surfaces and the Mohr–Coulomb model is adopted to describe their linear mechanical behaviour (Hao et al. 2015).

The FAI can be calculated for each type of joint. For type III joints, described by the Mohr–Coulomb criterion, FAI_{MC} is derived as follows (Feng et al. 2013):

$$\text{FAI}_{\text{MC}} = \begin{cases} \varpi_{\text{MC}}, & 0 \le \omega_{\text{MC}} < 1 \\ 1 + \text{FD}, & \text{FD} \ge 0 \end{cases} \tag{1}$$

$$\varpi_{\text{MC}} = 1 - \text{YAI}_{\text{MC}} \tag{2}$$

in which FD is the failure degree for the plastic zone, $\text{FD} = \frac{\overline{\gamma_{\text{p}}}}{\overline{\gamma_{\text{p}}^r}}$, in which $\overline{\gamma_{\text{p}}}$ is the equivalent plastic strain, and $\overline{\gamma_{\text{p}}^r}$ is the limit plastic strain; ϖ_{MC} is the complementary stress critical factor of the yield approach index YAI_{MC}, and

$$\text{YAI}_{\text{MC}} = \begin{cases} \dfrac{-\beta\tau_\pi}{\alpha\sigma_\pi + \gamma}, & \dfrac{\sigma_1 + \sigma_3}{2} \le \sigma_R \\ \dfrac{\sigma_1 - \sigma_R}{\sigma_L - \sigma_R}, & \dfrac{\sigma_1 + \sigma_3}{2} > \sigma_R \end{cases} \tag{3}$$

in which, σ_1, σ_3 are the maximum and minimum principal stresses; $\alpha = \frac{\sin\phi}{\sqrt{3}}$, $\gamma = -f\cos\phi$, in which f and ϕ are the cohesion and friction angle of the joints; σ_π and τ_π are the normal stress and shear stress on the π plane; $\beta = (\cos\theta_\sigma - \sin\theta_\sigma \sin\phi/\sqrt{3})/\sqrt{2}$ and θ_σ is the Lode angle;

$\sigma_R = \frac{\sigma_{\text{t}}(2-\sin\phi)-2f\cos\phi}{2-2\sin\phi}$ and $\sigma_{\text{t}} = \frac{f}{\tan\phi}$ is the ideal tensile strength; σ_L is the actual tensile strength.

However, the formula of FAI for the Barton-Bandis strength can be deduced as follows:

$$\tau = \sigma_{\text{n}} \tan\left[\phi_{\text{r}} + \text{JRClg}\left(\frac{\text{JCS}}{\sigma_{\text{n}}}\right)\right] \tag{4}$$

In which τ is the joint shear strength; σ_{n} is the normal stress on the joint; ϕ_{r} is the residual friction angle; JRC is the joint roughness coefficient, and JCS is the joint compressive strength. Then differentiation is applied to both sides of Eq. (4):

$$\frac{\partial\tau}{\partial\sigma_{\text{n}}} = f_a - f_b \tag{5}$$

In which

$$f_a = \tan\left[\phi_{\text{r}} + \text{JRClg}\left(\frac{\text{JCS}}{\sigma_{\text{n}}}\right)\right] \quad f_b = \frac{\pi \cdot \text{JRC}}{180\ln 10}\left(f_a^2 + 1\right) \tag{6}$$

For

$$\frac{\partial\tau}{\partial\sigma_{\text{n}}} = \tan\phi$$

Then

$$\phi = \arctan(f_a - f_b) \quad f = \sigma_{\text{n}} \cdot f_b \tag{7}$$

Substituting (6) and (7) into (3) gives:

$$\text{YAI}_{\text{bar}} = \begin{cases} \dfrac{-\beta_{\text{bar}}\tau_\pi}{\alpha_{\text{bar}}\sigma_\pi + \gamma_{\text{bar}}}, & \dfrac{\sigma_1 + \sigma_3}{2} \le \sigma_{\text{Rbar}} \\ \dfrac{\sigma_1 - \sigma_{\text{Rbar}}}{\sigma_L - \sigma_{\text{Rbar}}}, & \dfrac{\sigma_1 + \sigma_3}{2} > \sigma_{\text{Rbar}} \end{cases} \tag{8}$$

In which

$$\alpha_{\text{bar}} = \frac{f_a - f_b}{\sqrt{3}\left(f_a^2 + f_b^2 - 2f_af_b\right)} \quad \gamma_{\text{bar}} = -\frac{\sigma_n f_b}{f_a^2 + f_b^2 - 2f_af_b}$$

$$\beta_{\text{bar}} = \left[\cos\theta_\sigma - \sin\theta_\sigma \cdot \alpha_{\text{bar}}\right]\big/\sqrt{2}$$

$$\sigma_{\text{Rbar}} = \left[\sigma_{\text{t}}(2 - \alpha_{\text{bar}}) - 2\gamma_{\text{bar}}\right]\big/\left[2 - 2\sqrt{3}\alpha_{\text{bar}}\right]$$

$$\sigma_{\text{t}} = \sigma_{\text{n}}f_b/(f_a - f_b)$$

The FAI for the Barton–Bandis yield criterion, *i.e.* FAI_{bar} can then be obtained:

$$\text{FAI}_{\text{bar}} = \begin{cases} \varpi_{\text{bar}}, & 0 \le \omega_{\text{bar}} < 1 \\ 1 + \text{FD}, & \text{FD} \ge 0 \end{cases} \tag{9}$$

$$\varpi_{\text{bar}} = 1 - \text{YAI}_{\text{bar}} \tag{10}$$

In which ϖ_{bar} is the complementary stress critical factor of YAI_{bar}, and FD is the same as that proposed in Eq. (1).

Therefore, the FAI of types I and II joints can be calculated by putting φ_{rj1}, JRC_{j1}, JCS_{j1} and φ_{rj2}, JRC_{j2}, JCS_{j2}

into Eq. (9) respectively—in which, the φ_{rj1}, JRC_{j1}, JCS_{j1} are the residual friction angle, joint roughness coefficient and joint compressive strength of type I joints; the φ_{rj2}, JRC_{j2}, JCS_{j2} are the residual friction angle, joint roughness coefficients and joint compressive strength of type II joints. The FAI of the type III joints can be calculated by putting C_{j3}, φ_{j3} into Eq. (1), in which the C_{j3} and φ_{j3} are the cohesion and friction angle of type III joints. As the columnar jointed rock mass is aggregation function of these types of joints, the maximum FAI value of these three types of joints is taken as the FAI of the columnar jointed rock mass overall.

By using numerical analysis with input of the mechanical model and parameters, the FAI distribution of the columnar jointed rock mass can be obtained, see Fig. 8.

3.4 Determination of the EDZ for a Columnar Jointed Rock Mass

In numerical simulation, the depth of the EDZ can be determined by the FAI. Usually, the boundary of the EDZ is at FAI = 1. However, for columnar jointed rock masses under high stress and which suffer significant time-dependent cracking, the boundary of the EDZ becomes $0.8 < FAI < 1$. The extent of damage in the EDZ can be determined as the FAI value of the surface of the columnar jointed rock mass.

The in situ testing results for wave velocity and a digital borehole televiewer can also be used to recognize comprehensively the depth of the EDZ (Li et al. 2013a, b). It is indicated from Fig. 9 that, when the FAI = 1, the distance from the tunnel wall is 5.1 m. The acoustic velocity test results also indicated that the wave velocity was low within a depth of 5.1 m from the tunnel wall. In addition, the results of the borehole camera investigation also revealed that the cracking was distributed densely within the rock mass within a depth of 5.1 m from the tunnel wall. When the FAI = 1.8, the distance from the tunnel wall was 1.2 m, and the corresponding wave velocity was minimised and the cracking development was maximised. This showed that the FAI is a feasible indicator for evaluating the damage extent of EDZ of such columnar jointed rock mass.

3.5 Determination of the Threshold Value for the Allowable Damage Extent of the Columnar Jointed Rock Mass

The FAI indicates the extent of yielding in, or damage to, the surrounding rocks. If FAI = 1, the stress point is on the yield surface. So, yielding corresponds to the value FAI = 1. If the surrounding rock mass is damaged, it is within the EDZ, *i.e.* FAI ≥ 1. If the FAI is larger than the
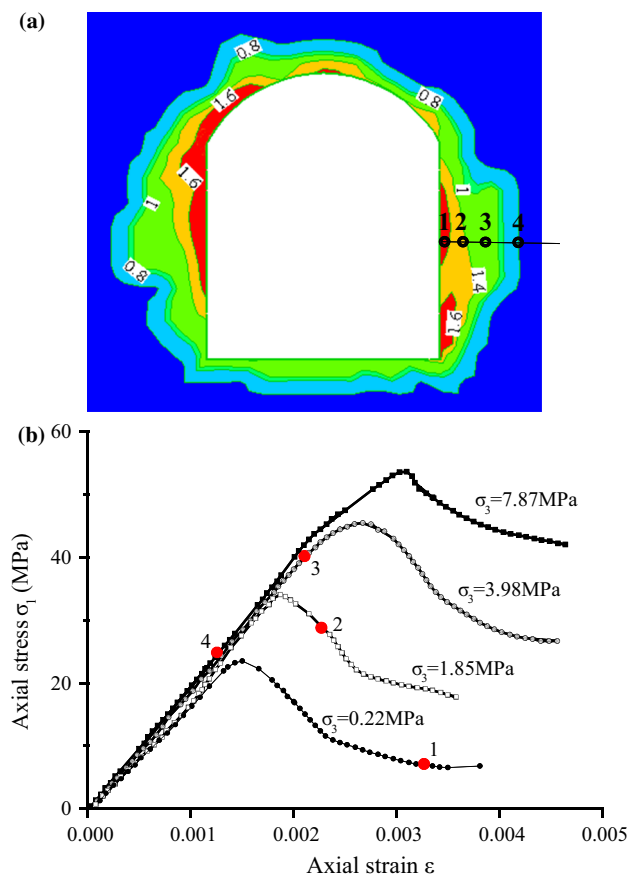

Fig. 8 a The extent of damage at different locations of the surrounding rock mass, indicated by the numerical values on the contour lines, and **b** the corresponding stress–strain curves. The corresponding point nos. *1*, *2*, *3* and *4* are indicated on the *dashed line* in (**a**)

threshold value of the allowable extent of damage, collapse may occur and support is needed to ensure tunnel stability. Therefore, the determination of the threshold value of the allowable extent of any damage extent is critical.

For the laboratory experiment, the threshold value of the allowable extent of damage was that corresponding to the point of structural failure along the stress–strain curves ("A", Fig. 10). This point could be determined by laboratory experiment and observation; however, it must be larger than that determined by field methods due to the scale effect. Therefore, only an approximate threshold value could be identified from this laboratory experiment at the design stage. Field investigation is also needed to assist in its determination.

The exact threshold value of the allowable extent of damage could be determined by back-analysis of the depth of collapse of the surrounding rock, which could be used to adjust the design of the support scheme during excavation. It can be seen from Fig. 11 that an allowable FAI is 1.36. The allowable FAI for a columnar jointed rock mass should

Fig. 9 a Extent of damage and
EDZ of the surrounding rock
measured by the P-wave
velocity and digital borehole
televiewer and b the relation
between the extent of damage
indicated by FAI and the
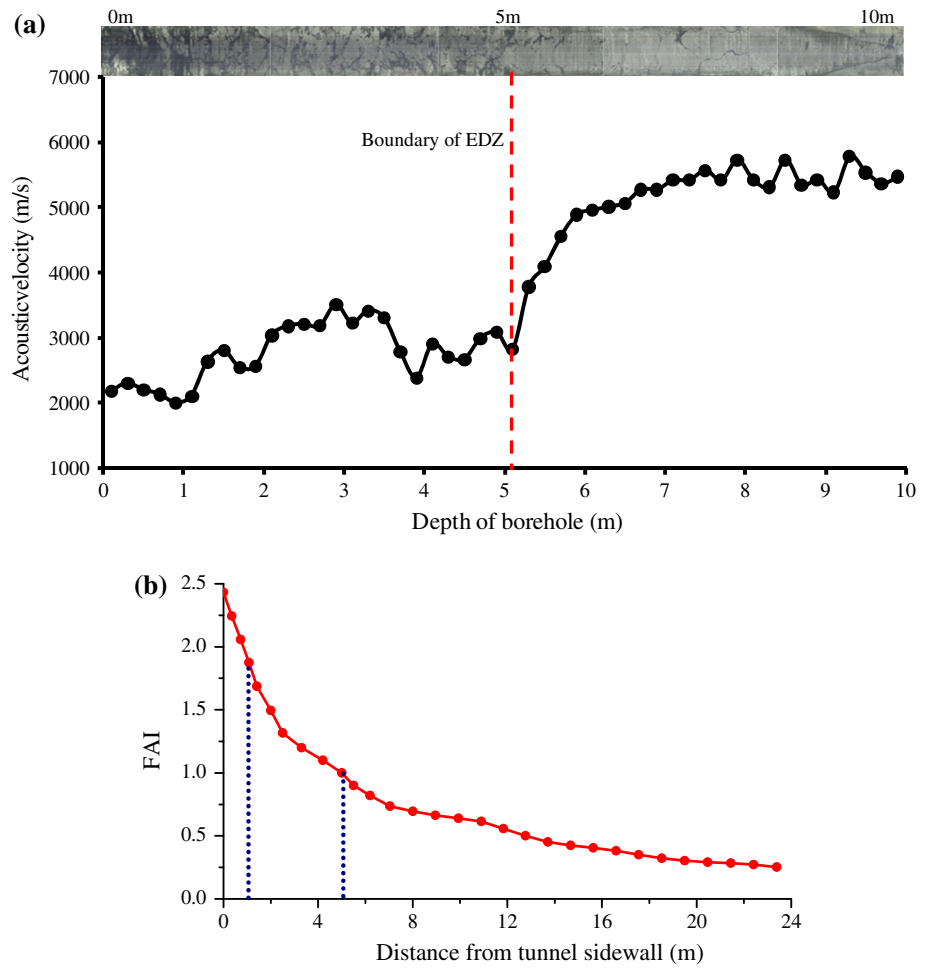distance from the tunnel
sidewall

Fig. 10 Determination method
of threshold value of the
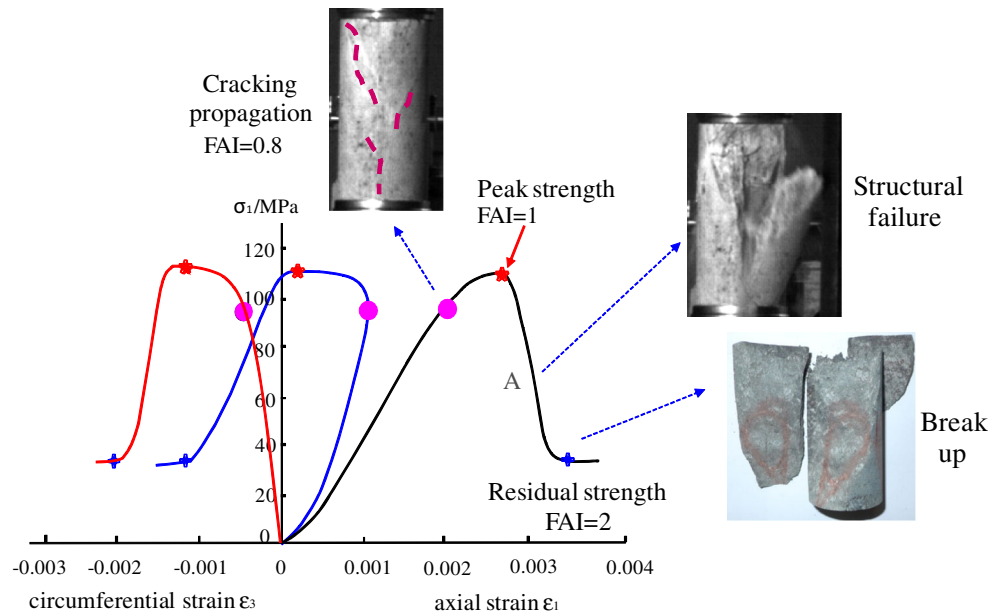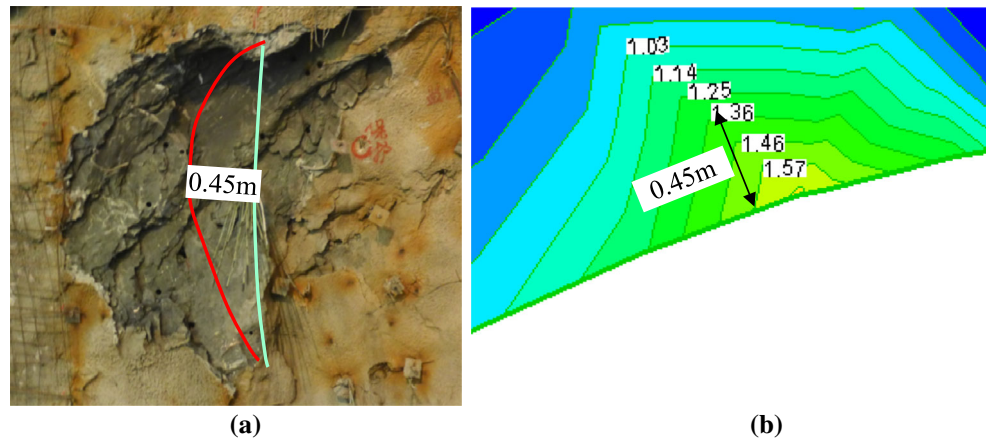allowable damage extent by
laboratory experiment

Fig. 11 Determination method of the threshold of damage extent of EDZ of surrounding rock: **a** depth of field damage and **b** the numerical analysis results indicated by FAI. FAI = 1.36 for the collapse depth of 0.45 m

(a)   (b)

be larger than 1 and smaller than 2, usually in the middle range of $1 \rightarrow 2$.

4 Determination and Verification of the Support Parameters Using the Cracking–Restraint Method

4.1 Determination of the Support Parameters

It is known that the rock properties measured in laboratory tests cannot be extrapolated directly to the field scale. Therefore, it is essential to compare numerical simulations with measurements obtained from long-term monitoring of such tunnels to acquire the properties of joints by back-analyses. Some properties of the columnar jointed rock mass which could be directly obtained from the laboratory and in situ testing are listed in Table 1, where E_1, E_2, v_1, and v_2 are the elastic moduli and Poisson's ratio of the basalt perpendicular and parallel to the column axis; G, C_0, ϕ_0, and σ_t are the shear modulus, cohesion, friction angle, and tensile strength of the basalt. The joint roughness coefficient JRC_{j1} and the residual friction angle of the jointing between columns φ_{rj1} was 6.35 and 20.06, as obtained by the back-analyses method.

4.1.1 Stress Analysis of the Excavation at each Stage

Staged-excavation of a cavern is a complex loading and unloading process. As shown in Fig. 12, the regions of

overstressing and unloading both exist after the excavation of a columnar jointed rock mass. For columnar jointed rock masses, the joint dip angle approaches the vertical, which leads to tensile failure on the tunnel sidewalls. It can be seen that the tensile failure of the joints mainly occurred at the surface of the surrounding rock and that shear failures mainly occurred within the surrounding rocks. The extent of such regions increases upon the excavation at each stage. The largest depth of the overstressed region is 6, 12, and 15 m for excavation stages 1, 2, and 3, respectively. There is no unloading region for the arch and bottom of the tunnel after the excavation of each stage; however, for the sidewall, the depth of the unloading regions is 1 and 2 m after the excavation of stages 2 and 3, respectively.

4.1.2 Determination of Shotcrete Thickness

The computational results for displacement and EDZ for different thicknesses of shotcrete in the diversion tunnels are shown in Fig. 13. Both the displacement and EDZ decreased with increasing thickness of shotcrete. However, the reduction in displacement was smaller than that for the EDZ. This indicated that shotcrete had a more significant effect on the EDZ than displacement. If the thickness of shotcrete was less than 100 mm, the inhibitory effect was not significant, either for the EDZ or displacement. However, if the thickness of shotcrete was greater than 100 mm, the displacement and EDZ would decrease slightly. Therefore, a reasonable thickness of shotcrete was deemed to be 100 mm.

Table 1 The parameters of the columnar jointed rock mass

Rock mass parameters	E_1 (GPa)	E_2 (GPa)	v_1	v_2	G (GPa)	C_0 (MPa)	φ_0 (°)	σ_t (MPa)
Values	10.5	8.6	0.26	0.26	8.63	6	37	1.5
Joint parameters	JCS_{j1} (MPa)	σ_{tj1} (MPa)	φ_{rj1} (°)	JRC_{j1}	JCS_{j2} (MPa)	σ_{tj2} (MPa)	φ_{rj2} (°)	JRC_{j2}
Values	125	0.22	32	13	125	0.10	20.06	6.35

(a) Stage 1   (b) Stage 2   (c) Stage 3

(a) Unloading regions of columnar jointed rock mass

(a) Stage 1   (b) Stage 2   (c) Stage 3

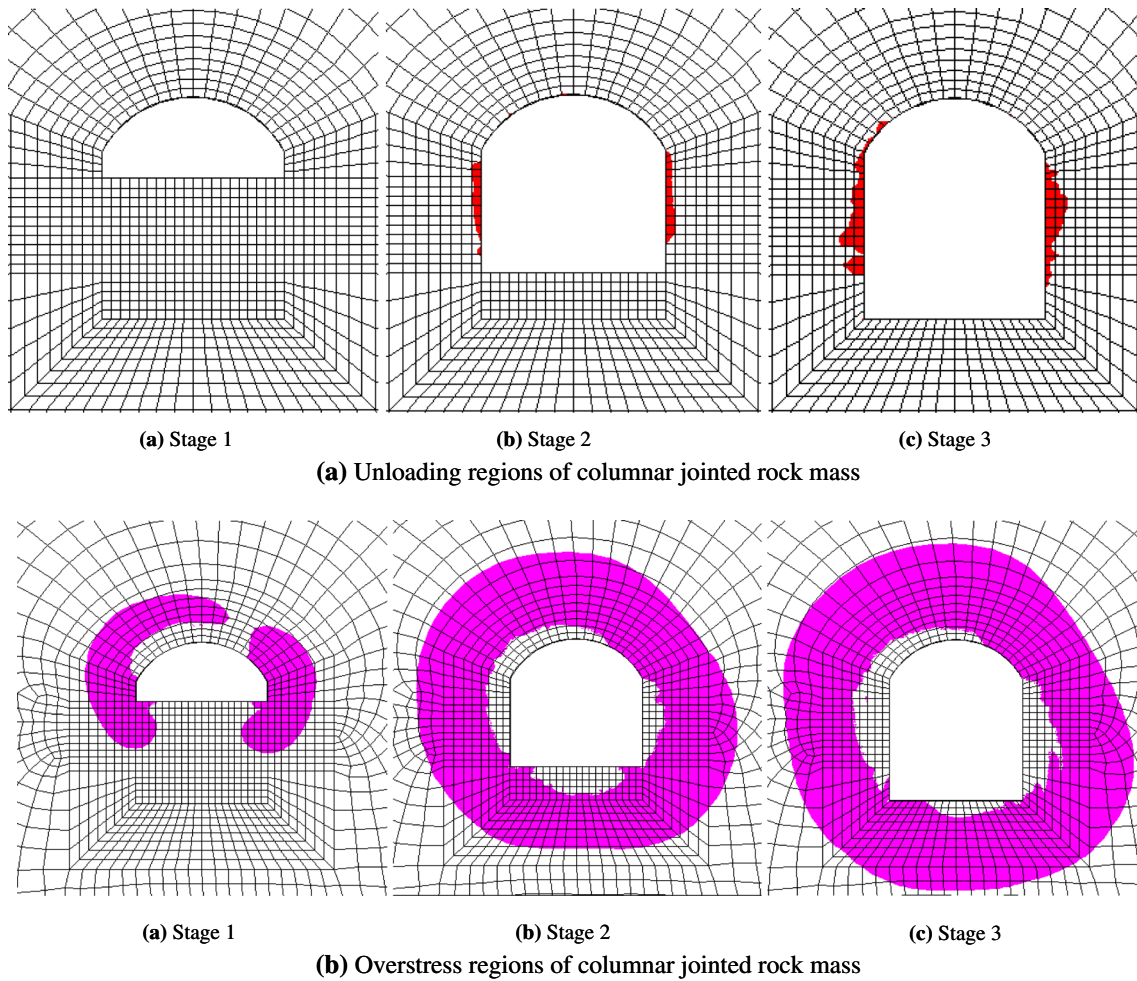**(b)** Overstress regions of columnar jointed rock mass

Fig. 12 Regions of over stressing and unloading of columnar jointed rock mass

4.1.3 Design of Rockbolt Support

(1)   Determination of the rockbolt length

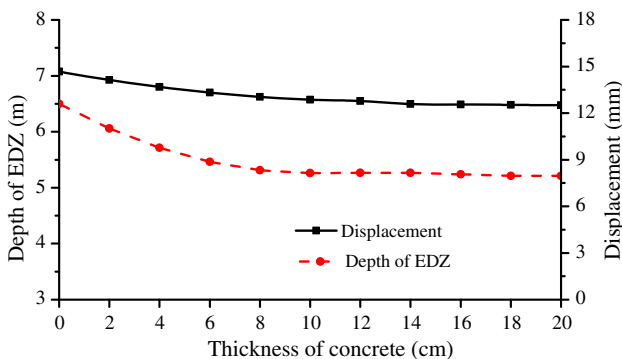Figure 14 shows typical results of a given section of tunnel. The diversion tunnels were designed with a service life of

Fig. 13 Computed displacement and EDZ versus thickness of shotcrete

7 years. The rockbolts should have enough length to control the unstable cracking expansion and post-peak cracking stages of the columnar joints according to the cracking-restraint method. The length of rockbolts should be greater than the contour line of FAI = 0.8.

Accordingly, as shown in the Fig. 14b, c, the length of rockbolts at the arch of the diversion tunnels should exceed 4.5 m and thus were set to 6 m; in the same way, the length of rockbolts is required to be larger than 5.6 m in the sidewall. Therefore, the length of rockbolts on the tunnel sidewalls was designed as 6 m. If collapse happens, the pre-stress anchor with length of 9 m could be used.

(2)   Determination of the installation angle of the rockbolts

For this columnar jointed rock mass, the joint dip angle approaches the vertical, which causes tension failure in the tunnel sidewall and shear failure in the tunnel arch. The function of rock bolts is not only to prevent the tensile failure of rock, but also to prevent its shear failure.
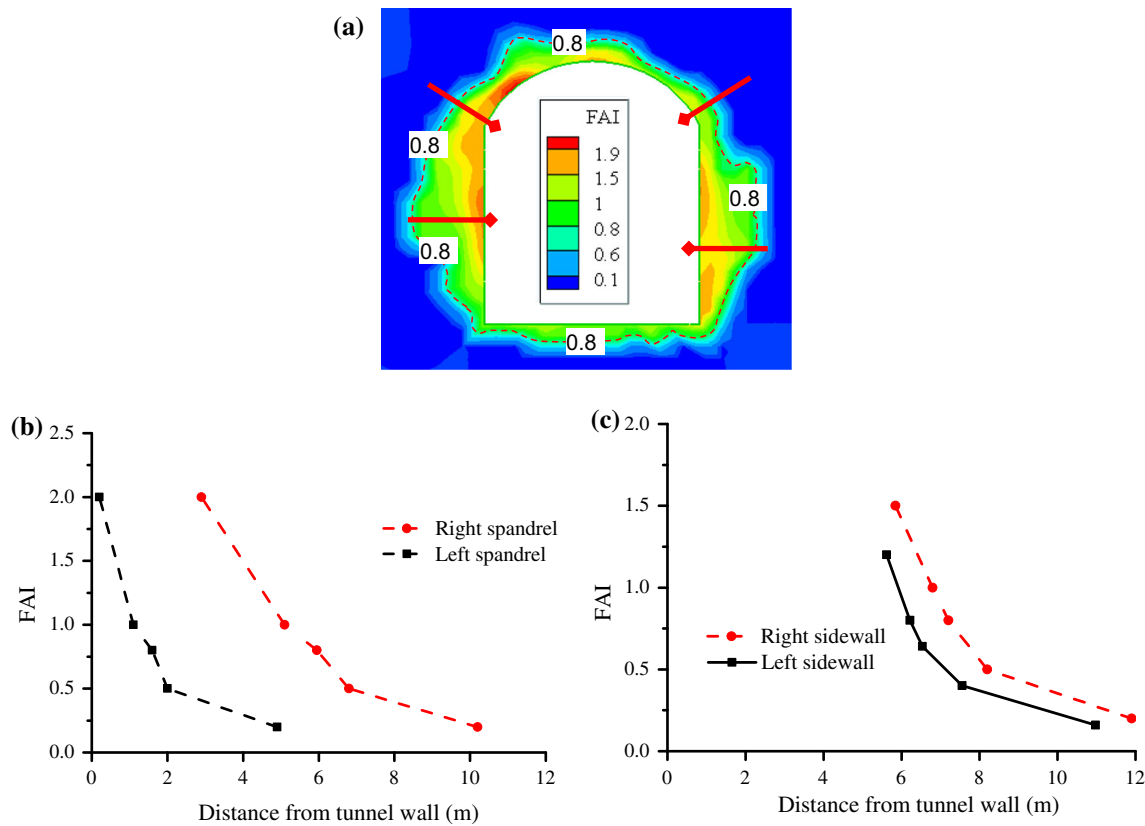
Fig. 14 a Extent of damage of a columnar jointed rock mass by numerical simulation, **b** depth of the EDZ in a columnar jointed rock mass measured by P-wave velocity, **c** design of bolt length for tunnel spandrel and **d** design of bolt length for tunnel sidewall

The relation between the depth of the EDZ and the angles of the rockbolts was studied to determine the optimal reinforcement angle for these rockbolts (Hirohisa and Hideto 2003; Al Hallak 2000) (see Fig. 15). The depth of the EDZ of the columnar jointed rock mass reaches its minimum if the rockbolts are installed perpendicularly to the main axis of the columnar jointed rock mass. This result is consistent with the support design principle of the cracking-restraint method. According to this method, the support was necessary to minimize the opening, cracking, and expansion of both joints and cracks. Therefore, the rockbolts should be installed in directions favourable to the control of the cracking and expansion of the joints (*i.e.*, in a direction normal to the main axis of the columnar joints as much as possible).

(3)   Determination of the spacing of rockbolts

The depth of the EDZ in the rock mass could be controlled by decreasing the spacing of rockbolts. However, as the spacing of rockbolts was reduced to a certain extent, the depth of the EDZ may have reduced slightly, but the cost of rock-bolting increases (De Buhan et al. 2008; Bernaud et al. 2009). This indicates that there is a reasonable bolt spacing that can ensure stability of the rock mass at

minimal cost. Figure 16 shows the influence of bolt spacing on the depth of the EDZ; this indicates that the depth of the EDZ has little changed as the bolt spacing was reduced to 1.2 m or less. Therefore, the most reasonable spacing of rockbolts for such a columnar jointed rock mass was recommended to be 1.2 m.

(4)   Determination of installation time for rockbolts

According to the support design principle of the cracking-restraint method, the support time of the rockbolts should ensure the stability of the rock mass. Moreover, the load acting on the anchor bolts should be sufficient to gain the best effect. Therefore, the depth of the EDZ, the FAI of the rock mass, and the axial stress in anchor bolts were calculated at different distances between the support location and the tunnel working face (see Fig. 17). As shown in Fig. 17, the depth of the EDZ increased with increasing distance from the supporting location to the tunnel working face. If the support distance was less than 20 m, the depth of the EDZ was logarithmically related to the support distance from the working face. If the distance was less than 40 m and larger than 20 m, the depth of the EDZ increased slowly. If the support distance exceeded 40 m, the depth of the EDZ increased significantly: the
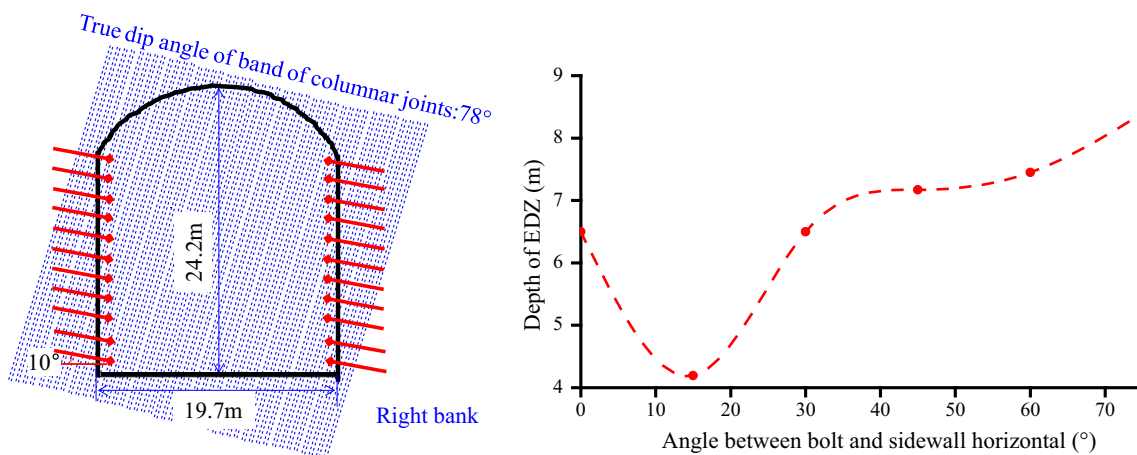
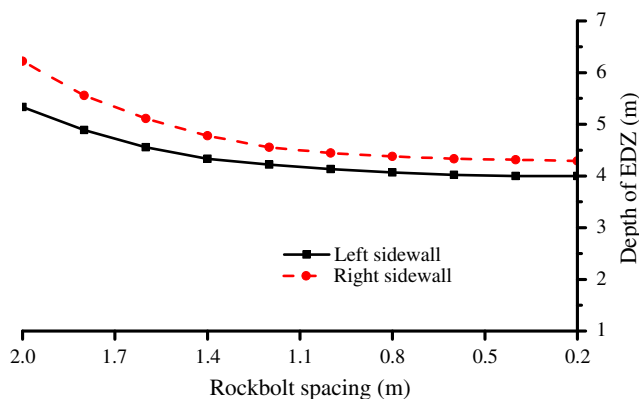Fig. 15 Influence of orientation of rockbolts on the depth of the EDZ

Fig. 16 Influence of spacing of rockbolts on the depth of the EDZ at tunnel sidewall

Fig. 17 Depth of the EDZ, load of rockbolts, and FAI for different locations from the support monitoring section to the tunnel working face

rock mass entered its accelerating stage and it became unstable.

According to the back analysis of the measured depth of collapse, the allowable FAI value should be 1.8, see Fig. 18. The FAI shows a consistent variation tendency with EDZ depth and, if the support distance exceeded 30 m, the FAI of the columnar jointed rock mass can exceed 1.8 and collapse may occur.

When the support distance was less than 5 m, the load acting on the anchor bolt exceeded the capability of the bolt. After that, the later the supporting time, the lower the load on rockbolts. When the support distance exceeded 30 m, the load on the bolt was too low, which indicated that the function of the rockbolts was not fully utilized.

In summary, according to the cracking-restraint method, the optimal support distance for this columnar jointed rock mass was 5–20 m. Moreover, the earlier the support, the less the final depth of EDZ of the rock mass, and the more effective the utilisation of bolt capacity. If the support distance was 20–30 m, the FAI and depth of the EDZ were
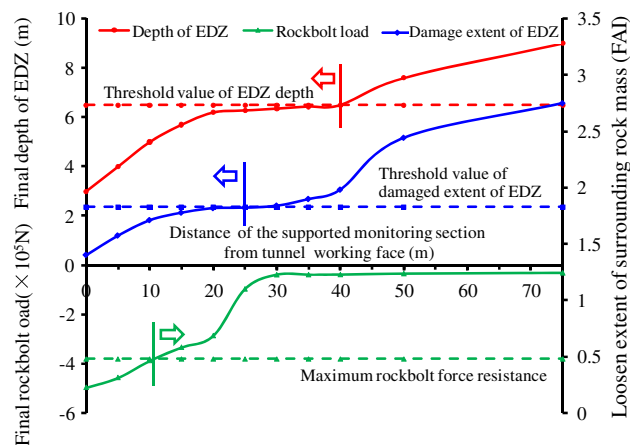
relatively large and the stability of the rock mass may be maintained. However, such support distances were unfavourable to long-term stability.

The final support parameters for the columnar jointed rock mass, as designed by the cracking-restraint method, are shown in Fig. 19.

4.2 Verification of the Support Design

4.2.1 Support Installation Following the Design

If the support parameters follow the design given by the cracking-restraint method, the FAI distribution of the diversion tunnel excavated in a columnar jointed rock mass is as shown in Fig. 20a. The extent of damage to the surface of the surrounding rock mass is 1.2, which is smaller than the threshold value determined by Fig. 18, i.e., 1.8, indicating that collapse will not occur. In addition, the

Fig. 18 Allowable damage extent of EDZ for columnar jointed rock mass: **a** depth of a collapse in columnar jointed rock mass, 1.5 m, and **b** FAI value evolution as distance from sidewall of tunnel. Allowable FAI = 1.8, that means allowable damage extent of surrounding rock shall be controlled
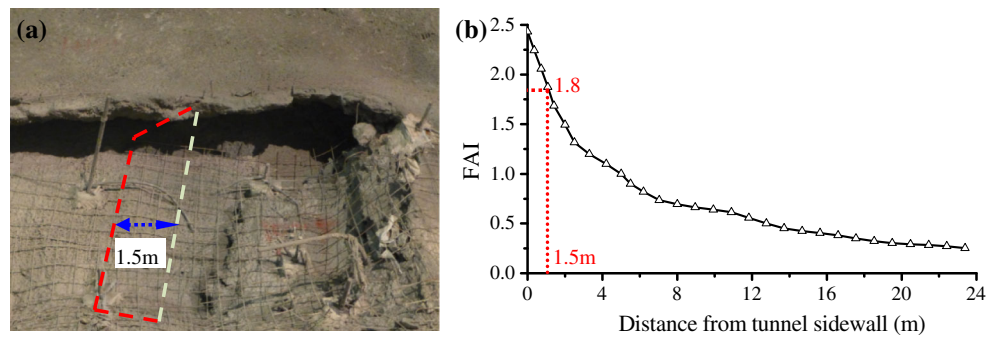
depth of the EDZ (FAI = 0.8) is also small, which indicates good tunnel stability.

Soon after the second layer, at chainage K0 + 320 in the No. 3 diversion tunnel on the right bank, was excavated on 6 January, 2013, the depth of EDZ was observed. The corresponding variation of depth of the EDZ is shown in Fig. 21. Before bolting, the depth of the EDZ increased rapidly; however, after bolting, the depth of the EDZ was stabilized within 1.5 m, which was shorter than the bolt length.

Therefore, the tunnel stability in such columnar jointed rock masses could be controlled if the support followed a design based on the cracking-restraint method (Fig. 22). These results proved the efficacy of the cracking restraint method.

4.2.2 Support Without Following Design

If the support parameters are designed and implemented as above, and the support time is later than that designed above, the FAI distribution is as shown in Fig. 20b. The extent of the damage to the surface of the surrounding rock

mass is 1.8, which indicates that collapse tends to happen. Furthermore, the depth of the EDZ is larger than that shown in Fig. 20a, exhibiting poorer tunnel stability.

The second layer at chainage K1 + 020 to K1 + 080 in the No. 5 diversion tunnel on the right bank was excavated on 2 January, 2013 (Fig. 23), and the surrounding rock was supported 2 months later. However, the depth of the EDZ kept increasing and experienced a sudden, rapid growth on 4 March, 2013. The rate of increase of the corresponding EDZ was also increasing, indicating that it had reached its accelerating cracking stage. After a further 20 days at this stage, collapse occurred in the columnar jointed rock mass.

5 Discussions

The commonest support design method is the convergence–confinement method and whether this CCM is appropriate for such a columnar jointed rock mass subjected to high stress warrants further discussion. If the convergence–confinement method was used to determine the optimal support time of a columnar jointed rock mass,

Fig. 19 Suggested support parameters for columnar jointed rock mass of tunnel using the method to restrain EDZ
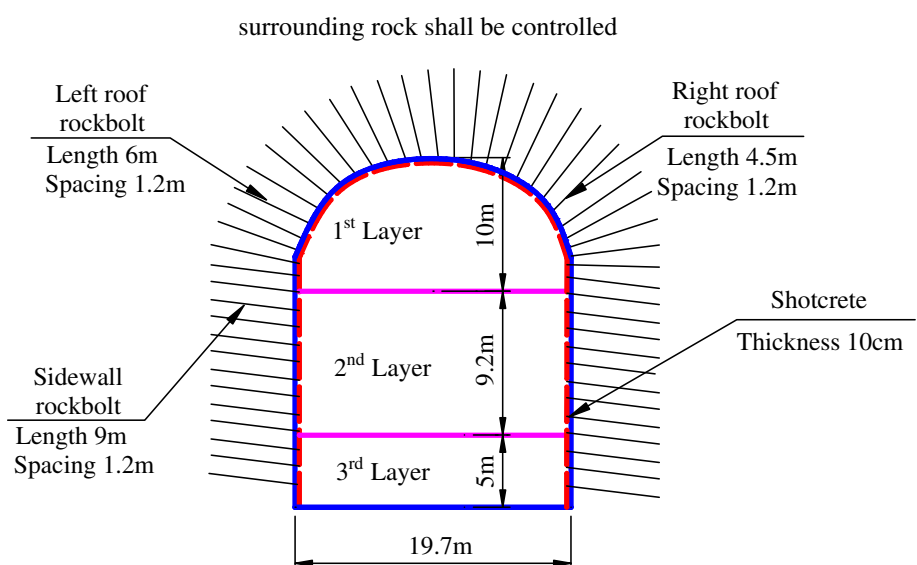
Fig. 20 FAI distribution of the diversion tunnel excavated in columnar jointed rock mass when the support parameters **a** follow the design given by the cracking-restraint method, and **b** did not follow the design
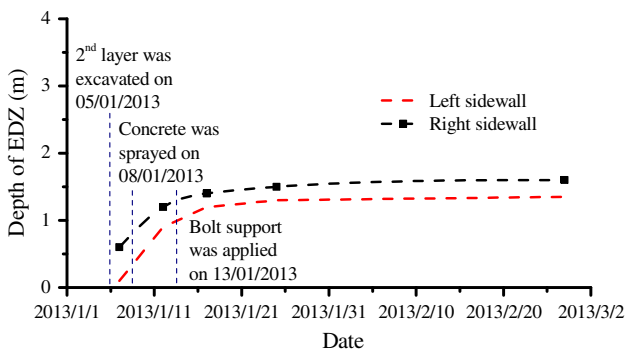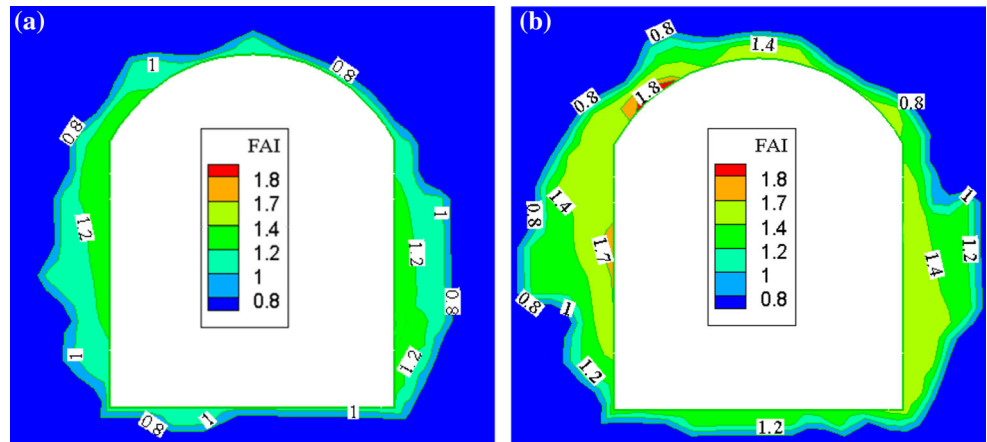

Fig. 21 Monitored time-dependent EDZ development with support parameters designed by the method to restrain EDZ

Fig. 22 Stability of tunnel sidewall at chainage K0 + 300 to K1 + 350 at No. 3 diversion tunnel with support parameters designed by the cracking restraint method
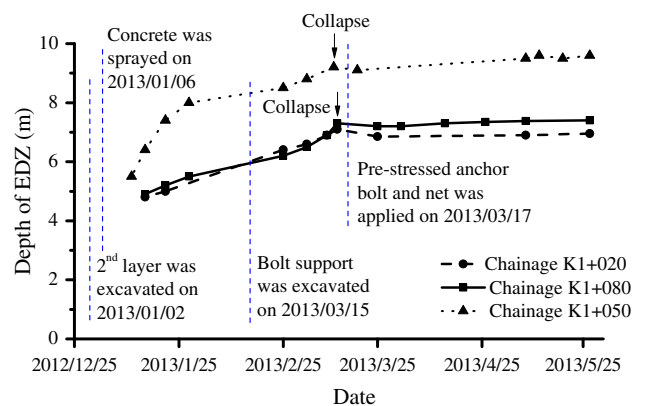

Fig. 23 Monitored time-dependent EDZ development of a tunnel section when the support parameters did not follow the design given by the method to restrain EDZ

Fig. 24 Support time determined by convergence-confinement method

the results are as shown in Fig. 24. The longitudinal deformation profiles (LDP) indicate that the influence zone ranges from −10 to 40 m; therefore, the optimal support time should be within this range. The ground characteristic
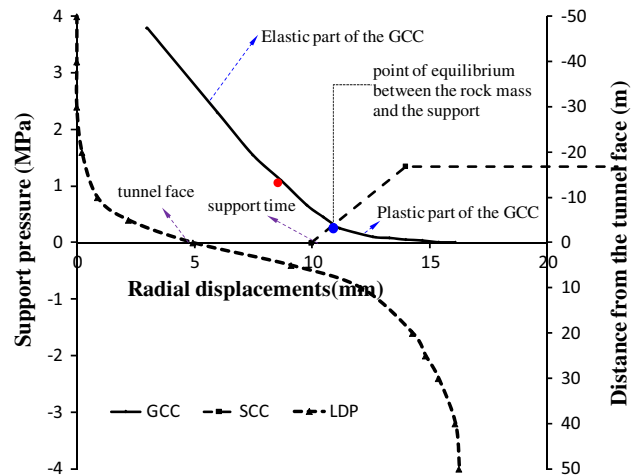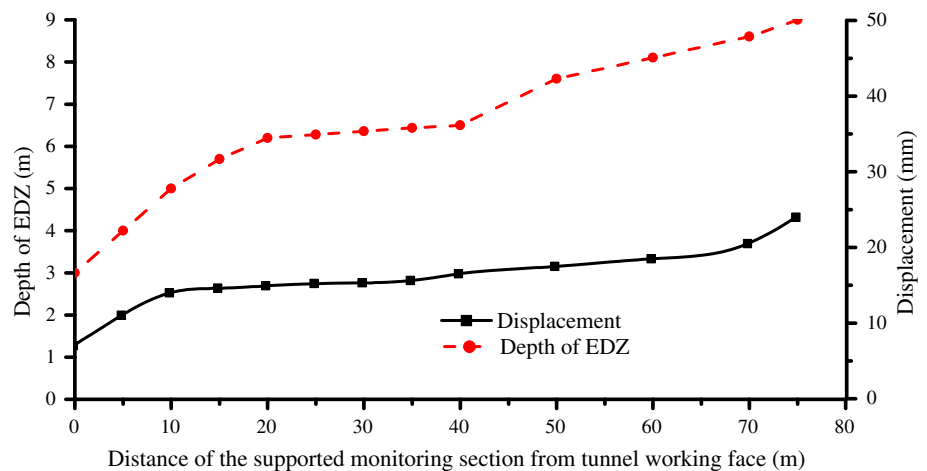
curve (GCC) and support characteristic curve (SCC) indicated that, if support was applied within 5 m after excavation, the support pressure would exceed that allowable

Fig. 25 EDZ depth and displacement for different locations from the support monitoring section and working face of the tunnel at Beihetan hydropower station

value; if the support were applied beyond 40 m, the displacement of the surrounding rock would exceed 16 mm, which was detrimental to tunnel stability. Therefore, the optimal support time ranged from 5 to 40 m after excavation.

Comparing this result with the cracking-restraint method, the optimal support time determined by the CCM was later, which may lead to support of the columnar jointed rock mass being delayed. If the support distance is larger than 20 m, although the displacement is small, the depth of the EDZ increased rapidly as shown in Fig. 25, which is bad for tunnel stability. For a columnar jointed rock mass, the high elastic modulus usually leads to small displacements, but the small displacements do not mean tunnel stability because the depth of the EDZ may increase. Therefore, the CCM is not appropriate for use in a columnar jointed rock mass subjected to high stress and the cracking restraint method, which reflects the essence of tunnel stability of columnar jointed rock mass, should be used to design the required supports.

6 Conclusions

The in situ measurements indicate development of cracking of a columnar jointed rock mass is a key issue resulting in reduction of strength and collapse subjected to high stress. The columnar jointed rock mass reveals also non-harmonious characteristics of deformation—with cracking evolution of the surrounding rock masses, such as small deformation before collapsing, or continuous increase of the EDZ depth, but stable slight deformation due to opening and closing of cracks.

The cracking-restraint method for support design has been developed to restrain the generation of new cracking, opening, expanding and connection of the existing and new cracks in the columnar jointed rock masses by

designing a reasonable support system. The design is for controlling the development of the excavation damaged zone and that of the damage extent in the EDZ of the columnar jointed rock masses. Not only the support parameters, such as thickness of shotcrete, spacing, length and arrangement of rockbolts, etc., but also the support time, such as the distance from the working face of time from the excavation, are determined.

The successful application of the developed design method in five diversion tunnels excavated in a columnar jointed rock mass at the Baihetan hydropower station, China, has indicated that it is an applicable and rational method for restraining cracking in such rock masses subjected to high stress.

References

Al Hallak R (2000) Experimental study of the stability of a tunnel face reinforced by bolts. Geotech Aspect Underground Constr Soft Ground, Balkema, Rotterdam, pp 65–68

Alejano LR, Alonso E, Rodríguez-Dono A et al (2010) Application of the convergence-confinement method to tunnels in rock masses exhibiting Hoek-Brown strain-softening behaviour. Int J Rock Mech Min Sci 47(1):150–160

Barton N, Løset F, Lien R et al (1981) Application of Q-system in design decisions concerning dimensions and appropriate support for underground installations. Subsurf Space 2:553–561

Bernaud D, Maghous S, De Buhan P et al (2009) A numerical approach for design of bolt-supported tunnels regarded as homogenized structures. Tunn Undergr Space Technol 24(5):533–546

Bhawani S, Viladkar MN, Samadhiya NK et al (1995) A semi-empirical method for the design of support systems in underground openings. Tunn Undergr Space Technol 10(3):375–383

Cai M, Kaiser PK (2005) Assessment of excavation damaged zone using a micromechanics model. Tunn Undergr Space Technol 20(4):301–310

Cai M, Kaiser PK, Tasaka Y et al (2004) Generalized crack initiation and crack damage stress thresholds of brittle rock masses near underground excavations. Int J Rock Mech Min Sci 41(5):833–847

Carranza-Torres C, Fairhurst C (2000) Application of convergence-confinement method of tunnel design to rock masses that satisfy the Hoek-Brown failure criterion. Tunn Undergr Space Technol 15(2):187–213

Chen BR, Feng XT, Zeng X et al (2011) Real-time microseismic monitoring and its characteristic analysis during TBM tunneling in deep-buried tunnel. Chin J Rock Mech Eng 30(2):275–283

Claudio O, Gunnar O (2004) Quality in tunnelling: ITA-AITES working group 16 final report. Tunn Undergr Space Technol 19(3):239–272

De Buhan P, Bourgeois E, Hassen G (2008) Numerical simulation of bolt supported tunnels by means of a multiphase model conceived as an improved homogenization procedure. Int J Numer Anal Methods 32(13):1597–1615

Feder G, Arwanitakis M (1976) Zur Gebirgsmechanik ausbruchsnaher Bereichetiefliegender Hohlraumbauten. BHM 121(4):103–117

Feng XT, Zhang CQ, Li SJ et al (2013) Dynamic design method for deep tunnels at hard rocks. Science Press, Beijing

Golshani A, Okui Y, Oda M et al (2006) A micromechanical model for brittle failure of rock and its relation to crack growth observed in triaxial compression tests of granite. Mech Mater 38(4):287–303

Gong QM, Zhao J, Jiang YS (2007) In situ TBM penetration tests and rock mass boreability analysis in hard rock tunnels. Tunn Undergr Space Technol 22(3):303–316

Hahn T, Holmgren J (1979) Adhesion of shotcrete to various types of rock surfaces and its influence on the strengthening function of shotcrete when applied on hard jointed rock. In: Proceedings, 4th international congress on rock mechanics, International Society for rock mechanics, vol 1, Montreux, Switzerland, pp 431–440

Hajiabdolmajid V, Kaiser PK, Martin CD (2002) Modelling brittle failure of rock. Int J Rock Mech Min Sci 39(6):731–741

Hao XJ, Feng XT, Yang CX et al (2015) Analysis of time-dependent EDZ development of columnar jointed rock mass in the Baihetan diversion tunnel. Rock Mech Rock Eng 48(9):1–24

Hirohisa K, Hideto M (2003) Centrifuge model test of tunnel face reinforcement by bolting. Tunn Undergr Space Technol 18:205–212

Hoek E, Martin CD (2014) Fracture initiation and propagation in intact rock—a review. J Rock Mech Geotech Eng 6(4):287–300

Horii H, Nemat-Nasser S (1986) Brittle failure in compression: splitting, faulting and brittle-ductile transition. Philos Trans R Soc Lond A: Math, Phys Eng Sci 319(1549):337–374

Jalalifar H, Mojedifar S, Sahebi AA (2014) Prediction of rock mass rating using fuzzy logic and multi-variable RMR regression model. Int J Rock Mech Min Sci 24(2):237–244

Jiang Q, Feng XT, Chen J, Huang K, Jiang YL (2013) Estimating in situ rock stress from spalling veins: a case study. Eng Geol 152(1):38–47

Jiang Q, Feng XT, Yossef HH et al (2014) Mechanical anisotropy of columnar jointed basalts: an example from the Baihetan hydropower station, China. Eng Geol 175:35–45

Kalman K (2003a) History of the sprayed shotcrete lining method—part I: milestones up to the 1960s. Tunn Undergr Space Technol 18(1):57–69

Kalman K (2003b) History of the sprayed shotcrete lining method—part II: milestones up to the 1960s. Tunn Undergr Space Technol 18(1):71–83

Kulatilake PHSW, Park J, Um J (2004) Estimation of rock mass strength and deformability in 3-D for a 30 m cube at a depth of 485 m at Äspö hard rock laboratory. Geotech Geol Eng 22(3):313–330

Li SJ, Feng XT, Li ZH et al (2012a) In situ monitoring of rockburst nucleation and evolution in the deeply buried tunnels of Jinping II hydropower station. Eng Geol 137(1):85–96

Li SJ, Feng XT, Li ZH et al (2012b) Evolution of fractures in the excavation damaged zone of a deeply buried tunnel during TBM construction. Int J Rock Mech Min Sci 55(10):125–138

Li SJ, Feng XT, Hudson JA (2013a) ISRM suggested method for measuring rock mass displacement using a sliding micrometer. Rock Mech Rock Eng 46(3):645–653

Li SJ, Feng XT, Wang CY et al (2013b) ISRM suggested method for rock fractures observations using a borehole digital optical televiewer. Rock Mech Rock Eng 46(3):635–644

Martin CD (1993) The strength of massive Lac du Bonnet granite around underground opening. Ph.D. thesis, University of Manitoba, 1993

Martin CD, Read RS, Martino JB (1997) Observations of brittle failure around a circular test tunnel. Int J Rock Mech Min Sci 34(7):1065–1073

Martin CD, Christiansson R, Söderhäll J (2001) Rock stability considerations for sitting and constructing a KBS-3 repository. Based on experiences from Äspö HRL, AECL's URL, tunneling and mining, SKB TR0138, Svensk Kärnbränslehantering AB

Martino JB, Chandler NA (2004) Excavation-induced damage studies at the underground research laboratory. Int J Rock Mech Min Sci 41(8):1413–1416

Pacher F (1964) Deformations messungen im Versuchsstollen als Mittel zurErforschung des Gebirgsverhaltens und zur Bemessung des Ausbaues, Felsmechanik, pp 149–161

Pan PZ, Yan F, Feng XT (2012) Modeling the cracking process of rocks from continuity to discontinuity using a cellular automaton. Comput Geosci 42:87–99

Wu FQ, Hu X, Gong M et al (2010) Unloading deformation during layered excavation for the underground powerhouse of Jinping I Hydropower Station, southwest China. Bull Eng Geol Environ 69(3):343–351